

The interaction of the DED magnetic field with a tokamak plasma

V.P. Zhukov¹ and K.H. Finken²

¹ Institute of Computational Technologies, Lavrentjeva Avenue, 6 Novosibirsk, 630090, Russia

² Institut für Plasmaphysik, Forschungszentrum Juelich GmbH, EURATOM Association, Trilateral Euregio Cluster, D-52425 Juelich, Germany

Received 10 November 2003, accepted for publication 28 April 2004

Published 28 May 2004

Online at stacks.iop.org/NF/44/S44

doi:10.1088/0029-5515/44/6/S05

Abstract

The penetration of the rotating magnetic field of the dynamic ergodic divertor (DED) into the TEXTOR tokamak plasma has been investigated, using a two-dimensional reduced magnetohydrodynamics model and taking into account the effects of plasma–neutral interaction and neoclassical viscosity. The real three-dimensional structure of the DED coils design results in a mixture of several spatial Fourier modes which rotate at different phase velocities. It is shown that the field penetration is accompanied by poloidal acceleration of the plasma, which plays a crucial role in the process. For the DED TEXTOR parameters, the plasma–neutral interaction and the neoclassical viscosity allow for a distribution of the perturbed magnetic field close to vacuum one. If the mixture of harmonics is taken into account, the acceleration of the plasma in poloidal direction does not provide a complete penetration of the perturbation.

PACS numbers: 52.35.Mw, 52.55.Rk, 52.30.-q

1. Introduction

The ac currents flowing in the coil system of the dynamic ergodic divertor (DED) of the TEXTOR tokamak produce helical magnetic perturbations that are resonant at different surfaces of the plasma. The main mode interacts with the $q = 3$ magnetic surface [1]. As a result of the interaction of the different modes the magnetic field on the tokamak edge is stochasticized. If one neglects induced plasma currents by the DED, the stochastic magnetic field is the superposition of the equilibrium field and the vacuum field produced by the DED coils. The properties of this field are studied in [2–8]. The influence of the plasma currents induced by the perturbation field and estimations of the torque to the plasma connected with DED fields earlier were studied in a linear approach [9–12]. Moreover, in [9–12], additional assumptions about resonance current sheet shape were used.

In this paper, the process of the penetration of the DED perturbations is studied numerically using a reduced (incompressible) magnetohydrodynamics (RMHD) model. It is shown that the rotating DED fields apply a torque to the plasma, and that the resulting plasma spin-up strongly affects the field penetration. This process cannot be described by a linear approach.

After a discussion of the DED coil modelling (section 2), we present the equations of the problem (section 3), discuss the

typical values of parameters for TEXTOR (section 4) and give results of the numerical modelling (section 5). The dependence of the magneto-plasma configuration on the amplitude of the DED current, of the friction connected with (a) the interaction of neutral impurities and (b) the neoclassical effects (magnetic pumping) will be discussed. Because the perturbation field consists of several spatial Fourier modes with different phase velocities, we also investigate this effect on the poloidal plasma acceleration. In section 6, we present results of the modelling of the device CSTN-IV and compare the results to those of a modelling of other authors [13, 14]. Finally, we will draw a conclusion.

2. The modelling of the DED coil system

In our modelling, we approximate the DED coils by a cylindrical system consisting of an infinitely long periodic cylinder with a poloidal angle $\varphi \in [0 : 2\pi]$ and the toroidal coordinate $z \in [0 : 2\pi R_0]$. The coils are placed on the radius r_c covering the poloidal angle φ lying in the interval

$$\left[\pi - \frac{\pi n}{m}, \pi + \frac{\pi n}{m} \right] \quad (2.1)$$

($n = 4, m = 12$) [12]. Each coil performs a single loop around the torus in a period along the z -axis (2.1).

In order to model the DED coils, it is convenient to consider a set of ml_0 ($l_0 = 4$) coils fully surrounding the tokamak. The coil number l crosses the plane $z = \text{constant}$ at the point

$$\varphi_l(z) = \frac{2\pi l}{ml_0} + \frac{zn}{mR_0}. \quad (2.2)$$

The finite poloidal width of the coil set is represented by equation (2.1) by introducing a form-factor g . The function $g(\varphi)$ is a step function, namely it equals 1 in the region (2.1) and is zero elsewhere.

Since the pitch angle of the coil is small, we consider only the z -component of the coil current. The vector potential for the vacuum solution is written as

$$\psi_c(r, \varphi, z, t) = -\frac{1}{2\pi} \sum_{l=1}^{ml_0} g(\varphi_l(z)) I_l w(\varphi - \varphi_l(z)). \quad (2.3)$$

Here $w(\xi) = \ln[(r_c^2 + r^2 - 2r_c r \cos(\xi))^{1/2}]$. The function $w(\varphi - \varphi_l)/(2\pi)$ corresponds to the vector potential of a single coil with coordinates r_c and φ_l . The current in the l th coil I_l is

$$I_l = I_0 \sin\left(\frac{2\pi l}{l_0} - \omega t\right). \quad (2.4)$$

Substituting (2.2), (2.4) into (2.3) we obtain

$$\begin{aligned} \psi_c(r, \varphi, z, t) = & -\frac{I_0}{2\pi} \sum_{l=1}^{ml_0} g\left(\frac{2\pi l}{ml_0} + \frac{zn}{mR_0}\right) \\ & \times \sin\left(\frac{2\pi l}{l_0} - \omega t\right) w\left(\varphi - \frac{2\pi l}{ml_0} - \frac{zn}{mR_0}\right). \end{aligned} \quad (2.5)$$

Let us consider the properties of equation (2.5). There it follows that

- (a) ψ_c is periodic in z with a period $2\pi R_0/n$,
- (b) for $g = 1$ —this corresponds to a set of coils fully surrounding the torus— ψ_c depends only on a value $\varphi - zn/(mR_0)$ and not on φ or z alone. Therefore, the problem is two-dimensional and periodic in φ with a period $2\pi/m$,
- (c) the expression (2.5) can be rewritten as

$$\begin{aligned} \psi_c(r, \varphi, z, t) \sim & \text{Im} \exp\left\{i\left(m\varphi - \frac{nz}{R_0} - \omega t\right)\right. \\ & \times \sum_{l=1}^{ml_0} g(\varphi - \xi_l) w(\xi_l) \exp(-im\xi_l)\left.\right\}. \end{aligned} \quad (2.6)$$

Here $\xi_l = \varphi - nz/(mR_0) - 2\pi l/(ml_0)$. In the limit $l_0 \rightarrow \infty$, the sum in (2.6) tends to an integral, which depends only on φ . The function w has a logarithmic singularities on the surface $r = r_c$. Because of this divergence, the convergence of the sum to the integral is the better, the larger the distance $|r - r_c|$ is. For the TEXTOR DED, both the number l_0 and the distance between plasma edge and coils position are sufficiently large and ψ_c at the plasma edge is well approximated by

$$\psi_c \approx \tilde{g}(\varphi) \sin\left(m\varphi - \frac{nz}{R_0} - \omega t\right). \quad (2.7)$$

Here $\tilde{g}(\varphi)$ is a function related to the above mentioned integral.

In the case of (2.7) the perturbation progresses along the z -direction with a phase velocity $R_0\omega/n$. For a plasma rotating in the z -direction, the perturbation can be treated as stationary. In the two-dimensional case, when $g = 1$, the function $\tilde{g} = \text{constant}$. Therefore, the perturbation (2.7) is treated as a rotation in the φ direction with the velocity $V_p = \omega/m$.

The perturbation of the magnetic field given by (2.7) exerts a force on the plasma mainly in the poloidal direction (φ direction) rather than in the z -direction. In the following, the plasma acceleration in poloidal direction and the influence of the poloidal plasma velocity on magnetic field penetration is investigated. The two-dimensional case in the limit $l_0 \rightarrow \infty$ will be considered. For simplicity, ψ_c is approximated by

$$\begin{aligned} \psi_c(r, \varphi, z, t) = & \psi_0\left(\frac{\varphi - nz}{mR_0} - V_p t\right), \\ \psi_0(\xi) = & -\frac{I_0}{2\pi} \sum_{l=1}^{ml_0} \sin\left(\frac{2\pi l}{l_0}\right) w\left(\xi - \frac{2\pi l}{ml_0}\right). \end{aligned} \quad (2.8)$$

Here ψ_0 corresponds to $\psi_c(r, \varphi, z = 0, t = 0)$ taken from expression (2.5).

We also try to understand how the three-dimensional geometry of the coils ($\tilde{g} \neq \text{constant}$) influences the poloidal (but not toroidal) plasma rotation. Below we model the effects of $\tilde{g} \neq \text{constant}$ using the two-dimensional model. For this we note that a major difference between the cases $\tilde{g} = \text{constant}$ and $\tilde{g} \neq \text{constant}$ is the generation of modes propagating with different poloidal velocities according to their mode number m . Therefore we use instead of equation (2.8):

$$\psi_c = \tilde{g}\left(\varphi - \frac{nz}{mR_0}\right) \psi_0\left(\varphi - \frac{nz}{mR_0} - V_p t\right). \quad (2.9)$$

The function (2.9) allows the transition to the two-dimensional case, using the coordinate $\varphi - zn/(mR_0)$. The perturbation (2.9) corresponds to a device that has another geometry than initial tokamak. Indeed, the function \tilde{g} is periodic with a period 2π . Therefore the expression (2.9) corresponds to a device with a period in z equal to $2\pi R = 2\pi R_0 m/n$. Respectively, the major tokamak radius in the case (2.9) is in m/n times larger than R_0 . The distribution (2.9) corresponds to a set of coils, which close after one loop in the toroidal direction. The current in the l th coil has a value $I_l = I_0 g(2\pi l/(ml_0)) \sin(2\pi l/l_0 - \omega t)$.

3. The mathematical formulation of the problem

We describe the plasma by the usual RMHD equations, which for the three-dimensional straight cylinder are written as [15, 16]

$$\begin{aligned} \frac{\partial A}{\partial t} + (\mathbf{V}\nabla)A &= H_z \frac{\partial \Phi}{\partial z} + \eta \nabla^2 A, \\ \rho \left(\frac{\partial \mathbf{V}}{\partial t} + (\mathbf{V}\nabla)\mathbf{V} \right) &= -\nabla p - (\nabla^2 A)\nabla A + H_z \frac{\partial \mathbf{H}}{\partial z} + \nu \nabla^2 \mathbf{V}, \\ \nabla \cdot \mathbf{V} &= 0, \\ \mathbf{V} \equiv (V_r, V_\varphi) &= \left(\frac{1}{r} \frac{\partial \Phi}{\partial \varphi}, -\frac{\partial \Phi}{\partial r} \right), \\ \mathbf{H} \equiv (H_r, H_\varphi) &= \left(\frac{1}{r} \frac{\partial A}{\partial \varphi}, -\frac{\partial A}{\partial r} \right). \end{aligned}$$

Here A is the z -component of the vector potential of the magnetic field and Φ is the stream function. This model assumes, that the z -component of the velocity is small, and the plasma density and the z -component of the magnetic field are constant:

$$V_z = 0, \quad H_z = \text{constant}, \quad \rho = \text{constant}.$$

Here, p is the sum of the plasma pressure and the gradient part of the magnetic field force. This value can be found using equation $\nabla \cdot \mathbf{V} = 0$. For a given resistivity η and viscosity ν , the knowledge of the plasma pressure is not required.

Below, a two-dimensional cylindrical model with a helical symmetry, i.e.

$$\frac{\partial}{\partial z} = -\frac{1}{aR} \frac{\partial}{\partial \varphi}, \quad R = \frac{R_0 m}{a n}$$

is considered. This symmetry coincides with the symmetry of the DED coils in the case $g = \text{constant}$. The direction of the helical direction (ignored in our equations) is close to magnetic field lines' direction, which results in a resonance surface in the two-dimensional problem. In the case of helical symmetry, all functions depend on $\xi = \varphi - z/(aR)$, but not on φ and z otherwise. It is convenient to introduce a coordinate $\varphi^* = \xi - V_p t$. For this coordinate, the coil perturbation (2.8) will be stationary. We stress that we do not make any transformation of the velocities. The velocity is the same as that in the laboratory frame. Below we remove the star. The RMHD equations in dimensionless form are written as

$$\frac{d\psi}{dt} = \eta \left(\Delta \psi - \frac{2}{R} \right), \quad (3.1)$$

$$\begin{aligned} \frac{dV_r}{dt} = & \frac{V_\varphi^2}{r} - \frac{\partial p}{\partial r} - \Delta \psi \frac{\partial \psi}{\partial r} \\ & + \nu \left(\Delta V_r - \frac{2}{r^2} \frac{\partial V_\varphi}{\partial \varphi} - \frac{V_r}{r^2} \right) - \mu_p V_r, \end{aligned} \quad (3.2)$$

$$\begin{aligned} \frac{dV_\varphi}{dt} = & -\frac{V_r V_\varphi}{r} - \frac{1}{r} \frac{\partial p}{\partial \varphi} - \Delta \psi \frac{1}{r} \frac{\partial \psi}{\partial \varphi} \\ & + \nu \left(\Delta V_\varphi + \frac{2}{r^2} \frac{\partial V_r}{\partial \varphi} - \frac{V_\varphi}{r^2} \right) - \mu_p V_\varphi - \mu_n \langle V_\varphi \rangle, \end{aligned} \quad (3.3)$$

$$\nabla \cdot \mathbf{V} = 0. \quad (3.4)$$

$$\mathbf{V} = (V_r, V_\varphi), \quad \Delta = \frac{1}{r} \frac{\partial}{\partial r} \left(r \frac{\partial}{\partial r} \right) + \frac{1}{r^2} \frac{\partial^2}{\partial \varphi^2},$$

$$\frac{d}{dt} = \frac{\partial}{\partial t} + V_r \frac{\partial}{\partial r} + \frac{(V_\varphi - r V_p)}{r} \frac{\partial}{\partial \varphi}.$$

Here ψ is the helical magnetic flux function. It is connected with the z -component of the vector potential as

$$\psi = A + \frac{r^2}{2R} H_z.$$

The components of the magnetic field are related to ψ by

$$H_r = r^{-1} \frac{\partial \psi}{\partial \varphi}, \quad H_s \equiv H_\varphi - \left(\frac{r}{R} \right) H_z = -\frac{\partial \psi}{\partial r}.$$

In equations (3.1)–(3.4), the following dimensionless variables are used: as a scale of length, we use the minor plasma

radius a ; for the magnetic field, we use the value of toroidal magnetic field H_z ; the velocity is normalized by the Alfvén velocity $V_A = H_z/(4\pi\rho)^{1/2}$ (here ρ is plasma density); the time is normalized by $t_a = a/V_A$; the pressure, by $H_z^2/(4\pi)$; the electric field, by $H_z V_A/c$ and so on.

In equations (3.1)–(3.4), the following transport processes are included: the resistivity η , the viscosity ν and the friction due to the interaction between plasma and neutral particles (charge exchange) μ_p and the friction connected with neoclassical effects (magnetic pumping) μ_n . We average the velocity over the poloidal angle $\langle V_\varphi \rangle = (2\pi)^{-1} \int_0^{2\pi} V_\varphi d\varphi$, because magnetic pumping [17] is not a local effect. The magnetic pumping appears from the rotation of the plasma around a minor tokamak cross section.

The initial conditions are:

$$\begin{aligned} V_r = V_\varphi = 0, \quad H_r = 0, \\ H_s \equiv -\frac{\partial \psi}{\partial r} = \left\{ \frac{m}{n} \frac{[1 - (1 - r^2)^{q_b+1}]}{q_b r^2} - 1 \right\} \frac{r}{R}. \end{aligned} \quad (3.5)$$

The parameter q_b corresponds to the q -factor at the plasma edge $r = 1$. According to equation (3.5), the magnetic field H_s changes its sign at the resonance surface $r = 1 - x_0$. The value q_b and the distance x_0 between resonance surface $q = m/n$ and the plasma edge are connected by (for $x_0 \ll a$)

$$q_b = \frac{m}{[n(1 - x_0/a)^2]}.$$

The equations (3.1)–(3.4) are solved in the region $0 < r < 1$. On the plasma edge $r = 1$, we require $V_r = V_\varphi = 0$ and a condition of a continuity of ψ and $\partial\psi/\partial r$ with a vacuum region in which the coils are placed. For the infinitely long, straight cylinder, the information about the coils' current is not sufficient for the determination of the ψ . It is necessary to put a special condition for zero harmonic of ψ in azimuthal direction. We apply the condition

$$\frac{1}{2\pi} \int_0^{2\pi} \psi d\varphi = -E_b t.$$

This corresponds to a constant electric field (loop voltage) E_b .

In order to solve the above problem, a finite-difference scheme is used. The boundary condition for the discrete analogue of ψ has the form (see appendix)

$$\begin{aligned} \psi_{i_0, j} = & -E_b t + \psi_{i_0-1, j} - \langle \psi_{i_0-1, j} \rangle + h_r \left(\frac{\partial \psi_c}{\partial r} - \left\langle \frac{\partial \psi_c}{\partial r} \right\rangle \right)_{i=i_0} \\ & + h_r \sum_{k=1}^{j_0} Q(k) (\psi_{c i_0, j+k} - \psi_{i_0, j+k}). \end{aligned} \quad (3.6)$$

Here

$$Q(0) = Q(j_0) = \frac{j_0}{4},$$

$$Q(k) = - \left(j_0 \sin^2 \left(\frac{\pi k}{j_0} \right) \right)^{-1} \quad \text{for } k = 1, 3, \dots, j_0 - 1,$$

$$Q(k) = 0 \quad \text{for } k = 2, 4, \dots, j_0 - 2.$$

$\psi_{i, j}$ is the value of ψ at the point (r_i, φ_j) . The point $i = i_0$ corresponds to the boundary: $r_{i_0} = 1$, $h_r = r_{i_0} - r_{i_0-1}$; $\varphi_j = 2\pi j/j_0$, $j = 1, \dots, j_0$.

For the case of a single phase velocity, the magnetic flux of the coil current in vacuum ψ_c (see equation (2.8)) becomes

$$\psi_c(\varphi) = -\frac{I_0}{2\pi} \sum_{l=1}^{m l_0} \sin\left(\frac{2\pi l}{l_0}\right) w\left(\varphi - \frac{2\pi l}{m l_0}\right). \quad (3.7)$$

In this case the problem is periodic in φ with a period $2\pi/m$, correspondingly, the calculation domain in poloidal direction is $0 < \varphi < 2\pi/m$.

For the mixture of the harmonics with different phase velocities (see equation (2.9)) we write

$$\psi_c = -\tilde{g}(\varphi + V_p t) \frac{I_0}{2\pi} \sum_{l=1}^{m l_0} \sin\left(\frac{2\pi l}{l_0}\right) w\left(\varphi - \frac{2\pi l}{m l_0}\right). \quad (3.8)$$

In order to reduce CPU time we take

$$\tilde{g}(\xi) = \left(\frac{1}{2}\right) \left(1 + \cos\left(\frac{m\xi}{M}\right)\right), \quad M = 3 \quad (3.9)$$

and respectively increase the calculation domain up to $0 < \varphi < 2\pi M/m$.

The above problem is solved by an implicit second-order-approximation finite-difference method. A non-uniform grid in r is used. In the region of the largest gradients ($r > 0.7$) the typical step of the grid in r was 0.0017. There are about eight grid points on each current peak shown in figures. To control the accuracy of the results, finer grids are applied as well.

4. The dimensionless parameters for TEXTOR DED

The typical TEXTOR parameters are as follows: the toroidal magnetic field $H_z = 25$ kGs; the plasma density near the wall is 10^{19} m^{-3} ; the minor tokamak radius $a = 47.7$ cm; the distance between the resonance surface and the plasma edge amounts to $x_0 = 5$ cm and the DED frequency 10 kHz. This gives $V_A = 1.74 \times 10^9 \text{ cm s}^{-1}$, $t_a = 2.7 \times 10^{-8} \text{ s}$, dimensionless frequency 1.7×10^{-3} . The dimensionless phase velocity for this frequency is

$$V_p = \frac{\omega}{m} \approx 1.4 \times 10^{-4}.$$

The dimensionless value of the current amplitude in the coil I_0 can be calculated using the formula

$$I_0 = \frac{I_0 \text{ (kA)}}{I_p \text{ (kA)}} \frac{2\pi}{q_b R_0}.$$

Here $I_0 \text{ (kA)} \approx 15 \text{ kA}$ is the current in the coil of DED TEXTOR in kiloamps, $I_p \text{ (kA)} \approx 600 \text{ kA}$ is the total TEXTOR plasma current in kiloamps, $(q_b R_0)^{-1}$ is the dimensionless value of the φ -component of the initial magnetic field on the boundary $r = 1$. It is assumed, that the dimensionless $H_z(r = 1) = 1$. For the dimensionless resistivity we use the following profile:

$$\eta = \min\left(\frac{E_b}{J_0(r)}, \eta_p\right) + \eta_b \exp\left(-\frac{(1-r)^2}{\delta^2}\right), \quad (4.1)$$

$$E_b = \eta_c J_0(r = 0).$$

Here η_c , η_p and η_b are the resistivity in the centre (core), near the resonance surface and close to the edge, E_b is electricfield

at the boundary (loop voltage), $J_0 = 2/R - \Delta\psi$ is initial plasma current.

The resistivity profile (4.1) has been chosen because the plasma motion is mostly determined by the resistivity in a narrow layer in the vicinity of the resonance surface η_p . For simplicity, $\eta_p = \text{constant}$ is taken where the value of the constant is determined by the Spitzer resistivity for the temperature at the resonance surface. The computational domain includes the plasma core region; this region is unperturbed by the DED magnetic field. However, the high resistivity η_p gives a very fast decay of the plasma core current. This is not physical; nevertheless, in order to keep the core current constant and at a reasonable value, the resistivity η_c is selected such that it corresponds to the Spitzer resistivity of TEXTOR at a core temperature of 1 keV. At the very edge, the plasma is cooler and the resistivity is much enhanced compared with η_p . Therefore, η is enhanced at the wall. Note that the exact value of $\eta_c \ll \eta_p$ and $\eta_b \gg \eta_p$ has only a minor influence on the calculation results.

The choice of profile (4.1) and of the value E_b allows us to keep the initial current in the plasma core, at the same time to have a given resistivity η_p in the region of resonance surface and finally the increased resistivity up to $\eta_b \gg \eta_p$ at δ near the wall.

The temperature of the plasma near the resonance surface is selected to 30–50 eV corresponding to a Spitzer resistivity of $\eta_p = 2\text{--}4.3 \times 10^{-7}$. In the calculations we put $\eta_b = 10^{-5} \gg \eta_p$, $\eta_c = 3 \times 10^{-8} \ll \eta_p$ and $\delta = 0.005$.

If the plasma velocity is larger than the diamagnetic velocity, the neoclassical friction coefficient has the following (dimensional) form [17]: $(1.5\tau_i v_{Ti}^2)/(qR_0)^2$. Here, τ_i is the ion collision time and v_{Ti} is thermal ion velocity. The Coulomb collision time for the TEXTOR edge plasma is $\tau_i \sim 5.3 \times 10^{-5} \text{ s}$, $v_{Ti}^2 \sim 3.5 \times 10^{-3} \text{ m}^2 \text{ s}^{-1}$. In the dimensionless form this becomes

$$\mu_n \sim 1.5 \frac{\tau_i}{t_a} \left(\frac{v_{Ti}}{V_A}\right)^2 \left(\frac{a}{q_b R_0}\right)^2 \sim 3.5 \times 10^{-3}. \quad (4.2)$$

Note, that the phase velocity and, respectively, the average plasma velocity of the TEXTOR DED can be either larger, or smaller, than the diamagnetic velocity [12].

The friction coefficient for the interaction of the plasma with neutral particles is much smaller than that of equation (4.2). The slowing down time of the plasma rotation is estimated to be 10^{-2} s [18]. In the dimensionless form this gives $\mu_p \sim 3 \times 10^{-6}$.

5. Results of the two-dimensional modelling

It is easy to see, that equations (3.1)–(3.4) have a stationary solution in which plasma co-rotates with the perturbation ($V_\varphi = r V_p$, $V_r = 0$) and the distribution of the magnetic field perturbation coincides with the vacuum one. It is also easy to see, that the penetration of the magnetic field perturbation into the plasma rotating with average velocity $\langle V_\varphi \rangle = r V_p$ is equivalent to the penetration of the static perturbation ($V_p = 0$) into an initially immobile plasma. It is clear that the penetration of a static magnetic field is sufficiently fast and complete.

For this reason we pay attention to the plasma acceleration (increasing of $\langle V_\varphi \rangle$). The following values are used:

$$v = \frac{1}{2\pi} \int_0^{2\pi} \frac{V_\varphi(r, \varphi)}{V_p} d\varphi, \quad h_r = \max_\varphi |H_r(r, \varphi)|,$$

$$h_s = \max_\varphi \left| H_s(r, \varphi) - \frac{1}{2\pi} \int_0^{2\pi} H_s(r, \varphi) d\varphi \right|,$$

$$j = \max_\varphi |J|.$$

Here $J = 2/R - \Delta\psi$ is the toroidal current. The values h_r^{vac} and h_s^{vac} analogous to h_r and h_s will be also used but for the coil magnetic field in vacuum. The region between the resonance surface (including the vicinity of the resonance surface) and plasma edge will be called the ‘periphery’.

First, we consider the perturbation of a *single phase velocity* (3.7) *without friction* ($\mu_p = \mu_n = 0$), $V_p = 1.4 \times 10^{-4}$ (the perturbation frequency is 10 kHz), $x_0 = 5$ cm, I_0 (kA)/ I_p (kA) = 15/600, $\eta_p = 3 \times 10^{-7}$, $\nu = 0.4\eta_p$. At the different moments of time, the flow is illustrated in the figures 1 and 2. One can distinguish three main reasons for plasma acceleration (increasing of $\langle V_\varphi \rangle$): (a) the skin current layer, (b) the current sheet at the resonance surface and (c) the slow acceleration of the plasma core due to viscosity. Due to the boundary condition $V_\varphi(r = 1) = 0$, one finds a thin layer where the plasma is decelerated.

The skin current layer appears at the very beginning (see figure 2(a)). It is formed at a small distance from the wall, because the resistivity increases strongly toward the wall. The skin current consists of two components. The first one is connected with the instantaneous increase of the coils’ current from zero to a finite value and, respectively, an abrupt increase in the magnetic field in the vacuum region near the plasma edge. At a small time step, this component of the skin current has a very large density, but is very thin. The second component of the skin current is connected with the periodicity of the coils current. Using the formula for the skin width in the dimensionless form $\delta = (2\eta_p/\omega)^{1/2}$, one obtains $\delta \sim 0.03$ and current density $\sim h_s^{\text{vac}}/\delta \sim 1$ for the parameters under discussion.

The numerical solution of equation (3.1) for an immobile plasma ($V_r = V_\varphi = 0$) shows that the lifetime of the first components of the skin current is about 200 Alfvén times. At $t \rightarrow \infty$ only the second component of skin current survives. It has a width $\delta \sim 0.02$ and current density ~ 1 .

The numerical solution of the linearized problem (3.1)–(3.6) shows, that the presence of the plasma makes the skin current at $t \rightarrow \infty$ (the second component of skin current) much smaller (about 0.15) than in the case of immobile plasma. The reduction of the second component of the skin current is connected with plasma motion. The magnetic field force in the skin layer pushes the plasma in such a manner that the current is decreased.

In the nonlinear case (the complete problem set in section 3), the plasma is accelerated as a whole (the increasing of $\langle V_\varphi \rangle$) in the skin. The mean azimuthal velocity $\langle V_\varphi \rangle$ grows quickly with increasing DED parameters. From figure 2(f) (curve 2) one can see that at $t = 165$, the mean azimuthal velocity $\langle V_\varphi \rangle$ at the plasma edge is close to V_p . The calculations show that the magnetic field penetrates much deeper into the plasma in the nonlinear case than in the linear

case ($\langle V_\varphi = 0 \rangle$). Note that the peak velocity of the skin current is significantly larger than the average one.

The current sheet at the resonance surface (see figures 1 and 2) becomes obvious at $t \sim 50$. The current density in this sheet achieves its maximum at $t \approx 120$. At this time, the skin current has already decreased significantly. In this phase, the magnetic field perturbation in the plasma is strongly shielded (see figures 2(c) and (d)).

The average azimuthal velocity $\langle V_\varphi \rangle$ increases very quickly in the current sheet (see figure 2(f)). Note, that not average velocity on the stage of resonance current sheet is significantly larger than average one at this stage (see figure 1(a)).

From then on, the plasma periphery continues to accelerate up to the velocity rV_p . When the periphery plasma velocity becomes close to rV_p ($t \sim 4 \times 10^4$) the plasma current becomes small and the distribution of the magnetic field perturbation practically coincides with a vacuum one (see figures 2(c) and (d)).

The acceleration of the plasma at the core takes much longer than at the plasma periphery. This is because a proper plasma acceleration force (the perturbation of the current) is missing at the core. The core is accelerated due to viscous moment transport. In addition, the acceleration force is also small on the periphery on a longer timescale. Note, that in our calculations the plasma density is constant in the computational domain. In reality the plasma density at the core is much larger than at the periphery. This additionally decreases the core acceleration.

For $t \rightarrow \infty$ the difference between V_φ and $\langle V_\varphi \rangle$ becomes small everywhere, except a thin boundary layer near $r = 1$ where the velocity V_φ can be significantly larger V_p (see figure 2(e)). This is connected with the boundary condition $V_\varphi(r = 1) = 0$. Because of this condition there is no complete compensation of skin current by the plasma rotation. The calculations show, that for a ‘slipping’ boundary condition ($\partial(V_\varphi/r)/\partial r|_{r=1} = 0$) the difference $V_\varphi - rV_p$ tends to zero in time everywhere in calculation domain.

It is necessary to emphasize that in the DED TEXTOR case the plasma acceleration and magnetic field penetration take several hundreds of Alfvén times. This is much smaller than the period of the coils’ current $2\pi/\omega = 3400$ Alfvén times (for 10 kHz). Therefore, a linear theory or the methods developed in [12, 19] cannot be applied directly in the analysis of the problem. Note, that in [12, 19] the equation connecting the torque to the dissipated power is used. In order to obtain this equation the relation $\partial/\partial t = -(\omega/m)\partial/\partial\varphi$ is used. This relation is applicable only for slow changes of average values, i.e. for small DED coils’ current. The method developed in [12, 19] can be used also for the description of the quasisteady stage of the motion. Note, that for long times the time average coincides with the averaging over the angle φ . Therefore, φ in (3.1)–(3.4) corresponds to $\xi - V_p t$.

Due to the strong nonlinearity, the average velocity $\langle V_\varphi \rangle$ slightly exceeds V_p and is slightly negative at some times and radii (see figure 2(f)). The calculations show that the smaller the amplitude of the coils current smaller are these effects.

The estimation based on the calculation results show that the plasma temperature in the skin layer and in the resonance current sheet can increase substantially. The heat conductivity

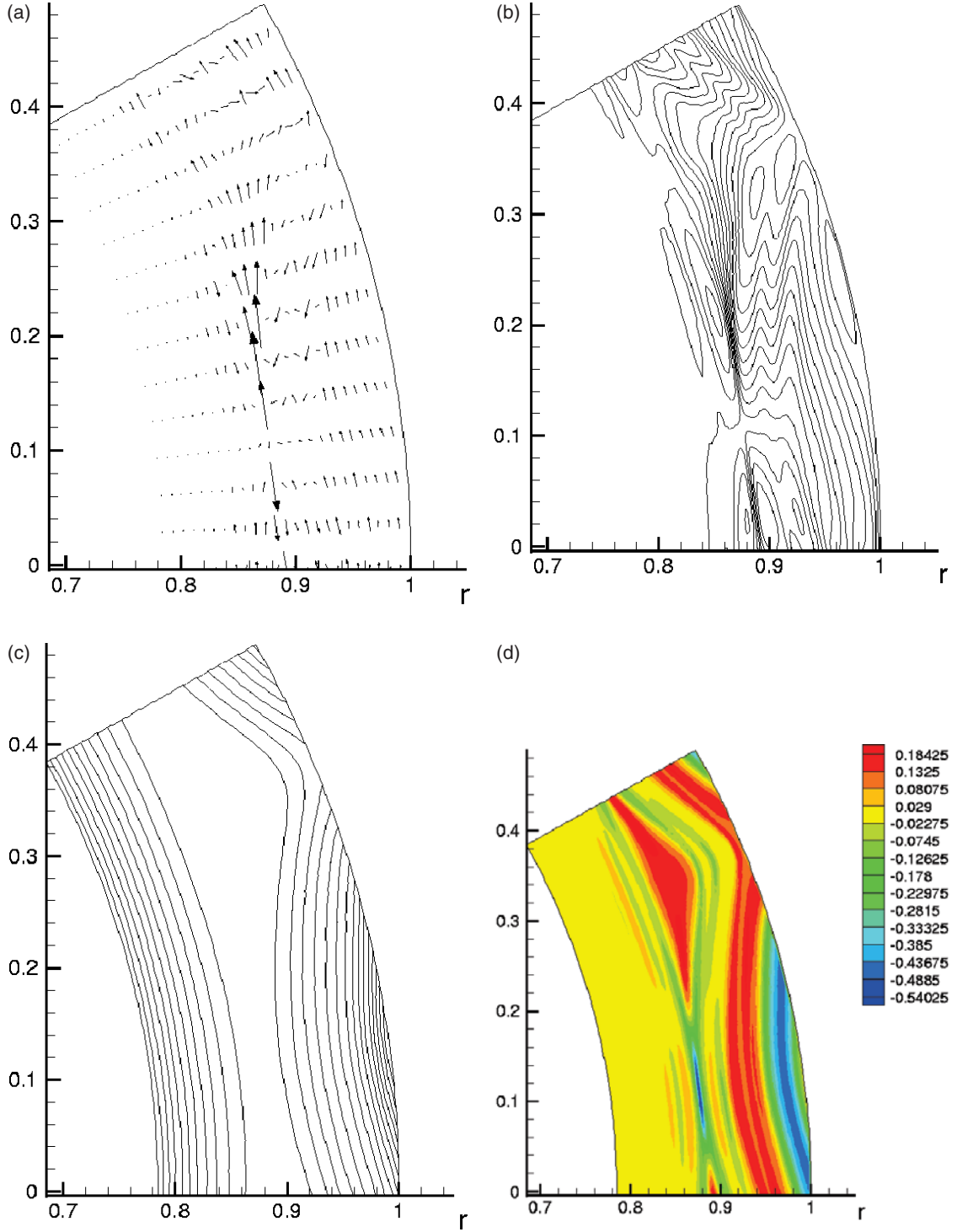


Figure 1. (a) The velocity field ($\max |V| \sim 10V_p$), (b) the stream function, (c) the magnetic field lines (isolines of ψ), (d) the toroidal current J at $t = 170$. The case of single harmonic, $\mu_p = \mu_n = 0$, $V_p = 1.4 \times 10^{-4}$ (the perturbation frequency is 10 kHz), I_0 (kA)/ I_p (kA) = 15/600, $\eta_p = 3 \times 10^{-7}$, $\nu = 0.4\eta_p$.

parallel to the magnetic field also plays an important role, because some magnetic flux tubes cross the cold wall during their motion (see figure 1(c)). In the limit of large toroidal magnetic field and slow (in comparison to t_a) motion, the temperature dependence of the resistivity influences the plasma motion. In our modelling, the resistivity is assumed to be constant. The temperature effects are beyond the scope

of our article. We can only note that the calculations with different values of resistivity show that the value of the resistivity does not change the picture of the motion qualitatively. Some quantitative differences, however, are observed.

Note also that the calculated fast acceleration of the plasma in the skin layer may be incompatible with the actual power

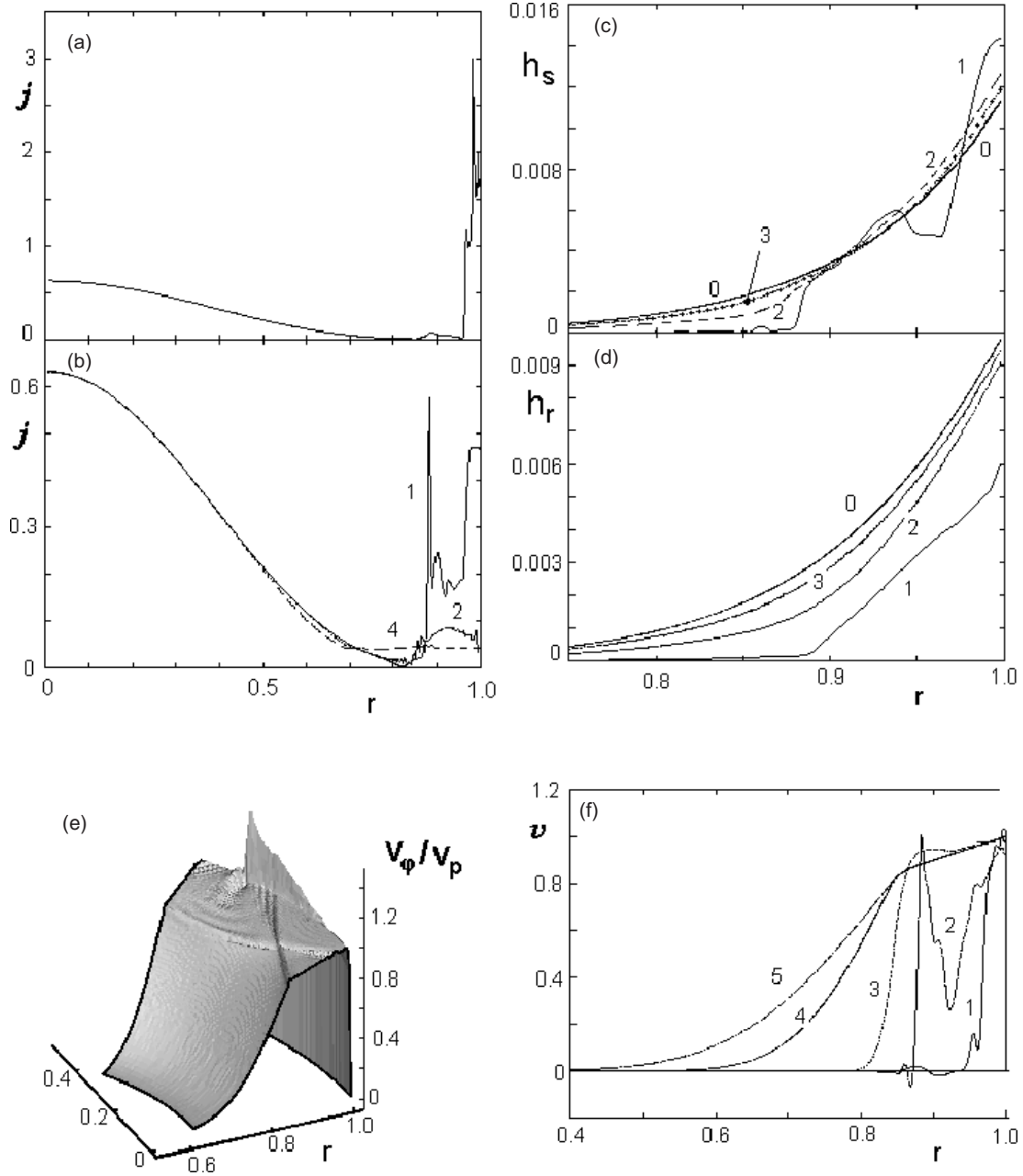


Figure 2. (a) The distribution of j at $t = 30$, (b) the distribution of j , (c) h_s , (d) h_r , (f) v for different time moments and (e) the distribution of V_ϕ/V_p at $t = 10^5$. Curves 1, 2, 3 and 4 on the plates (b), (c), (d) correspond to the time moments $t = 165, 3100, 1.2 \times 10^4$ and 4.6×10^4 , respectively. Curves 0 correspond to (c) h_s^{vac} , (d) h_r^{vac} . Curves 1, 2, 3, 4 and 5 on the plate (e) correspond to the time moments $t = 40, 165, 3100, 4.6 \times 10^4, 1.1 \times 10^5$. The parameters are the same as for figure 1.

supply of the DED. In the calculations it is assumed that coil current reaches its amplitude abruptly. The gradual increase of the coil current does not change the picture qualitatively. Only the amplitudes of the skin-current and current on the resonance surface will be smaller. Respectively, the time of plasma acceleration and the magnetic field penetration will be larger.

The reduced coil current ($I_0 = 5$ kA instead of $I_0 = 15$ kA) does not change the picture qualitatively. However, quantitatively, the process of acceleration and penetration for $I_0 = 5$ kA is approximately ten times slower than for $I_0 = 15$ kA. This results from the fact that the penetration process is connected with plasma acceleration;

it should depend quadratically on the amplitude of the coil current.

The friction coefficients $\mu_p, \mu_n < 0.1$ have no significant influence on the motion for $I_0 = 15$ kA. The only effect is that even a very small friction (for example $\mu_p = 10^{-6}$) prevents the plasma core from spinning up. As a result, the stationary solution is established similar to the case without friction; however, the plasma core is immobile. This means, for the TEXTOR DED, that the magnetic pumping and charge exchange effect prevent a substantial plasma rotation in the core, but does not reduce the poloidal acceleration of the plasma periphery and magnetic field penetration in the two-dimensional RMHD model.

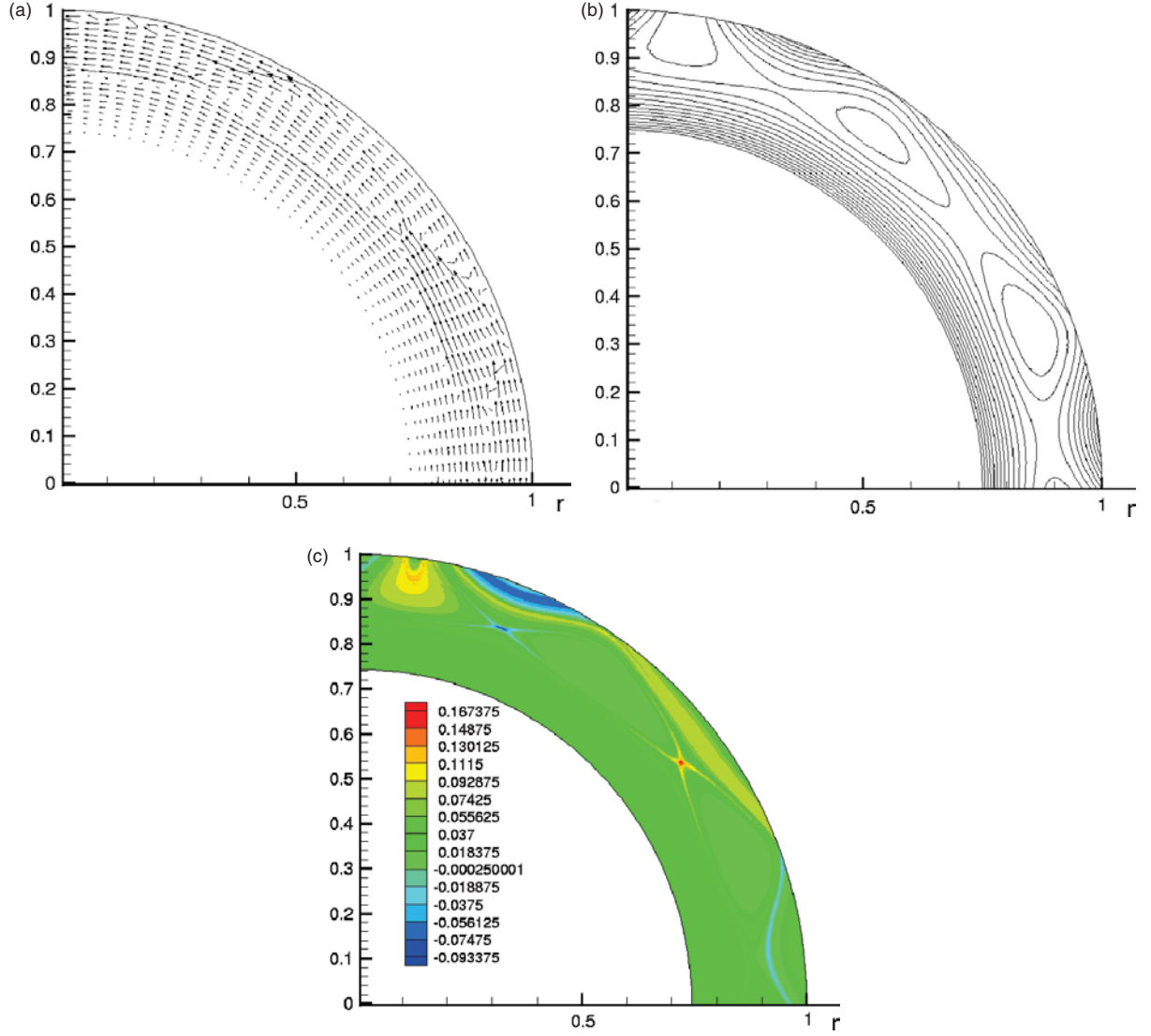


Figure 3. The case of mixture of harmonics at $t = 23\,070$; (a) velocity field ($\max |V| \sim 4.3V_p$), (b) the magnetic field lines (isolines of ψ), (c) the current J distribution.

Only for very large friction coefficients $\mu_p, \mu_n \sim 5$, the situation changes. For $\mu_n = 0, \mu_p = 5$ the skin-current near $r = 1$ does not decay. The current sheet at the resonance surface is not formed. The plasma moves only near the edge $r = 1$ with a velocity slightly larger than V_p . The average velocity in this area remains smaller than V_p . The magnetic perturbation field inside the plasma is significantly smaller than in vacuum case. The motion in the case $\mu_n = 5, \mu_p = 0$ is significantly different from that for $\mu_n = 0, \mu_p = 5$. In this case, the initial phase is similar to that of $\mu_n = 0$. However, the average plasma velocity can not spin up to V_p . Therefore, the current perturbation on the periphery does not decay. The plasma remains far from the equilibrium in which it co-rotates with phase velocity. This results in a strong shielding of the magnetic field. The large current density in the vicinity of the magnetic field separatrix (the line which divides the region of closed and open magnetic flux tubes) takes place. There are strong vortices around the islands of magnetic field. The plasma velocity in the vortices is much larger than V_p . The solution for $\mu_n = 5, \mu_p = 0$ does

not lead to a stationary state. At large times, one observes irregular oscillations with varying amplitude and period (the time interval between maxima) ~ 200 Alfvén times. However, these cases are not relevant for TEXTOR.

The influence of μ_p increases for small I_0 . Therefore, the friction force becomes significant when the friction force value $\mu_p V_p$ is comparable to the average force $\langle \Delta \psi r^{-1} \partial \psi / \partial \varphi \rangle$, which is proportional to I_0^2 . For this reason, the friction with much smaller amplitude of perturbation than for the TEXTOR DED can play significant role; it may be relevant for the problem of an error-field [20].

Figures 3–5 treat the case of a mixture of harmonics (3.8) and (3.9). The beginning of the motion is similar to the case of perturbation with a single phase velocity (3.7). However, the function ψ_c of equations (3.8) and (3.9) has the property

$$\psi_c(\varphi - V_p t, t + T) = \psi_c(\varphi, t), \quad T = \frac{2\pi}{mV_p}. \quad (5.1)$$

After a long time, a flow close to a flow with the symmetry (5.1) is established. All functions on the periphery change significantly in time.

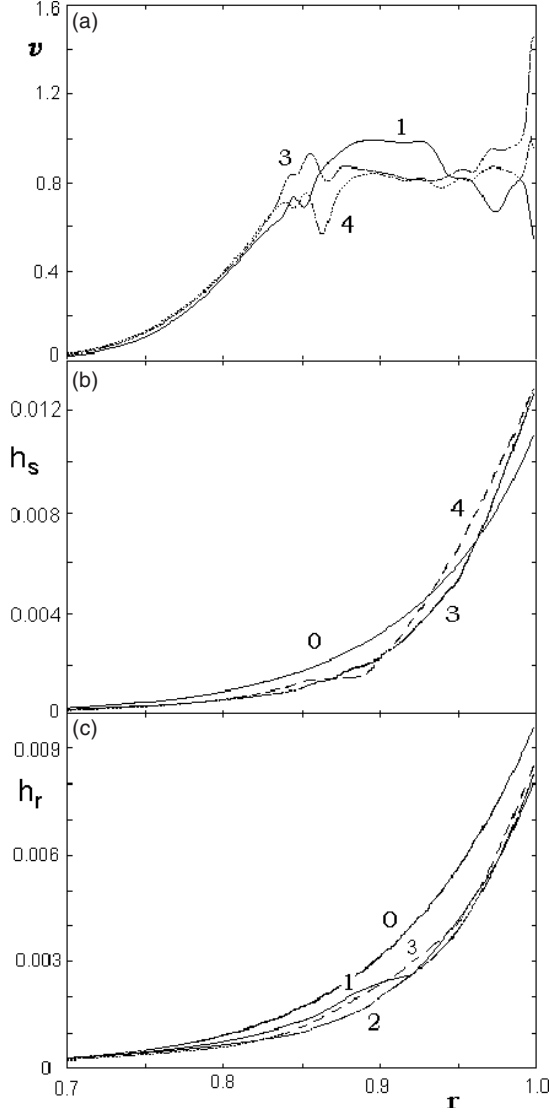


Figure 4. The distribution of (a) v , (b) h_s , (c) h_r for the case of mixture of harmonics in different moments of time. Curves 1, 2, 3 and 4 correspond to the time moment $t = 20\,265, 21\,200, 22\,135, 23\,070$, respectively. These moments of time belong to one period. The curves 0 on (b) and (c) correspond to h_s^{vac} and h_r^{vac} .

The perturbation of the electrical current on the periphery is not small. There are current peaks in the X-points. The current density is also large in the vicinity of the magnetic field separatrix and in the magnetic island, which is in contact with plasma boundary $r = 1$ (the up-left part of the figure 3(c)). The current density in other region is small, including magnetic islands which are isolated from the boundary. The difference between the magnetic field perturbation in the plasma and the magnetic field perturbation in vacuum is significant.

6. The modelling of the CSTN-IV tokamak

In this section, we discuss the solution of the problem for the parameters corresponding to the tokamak CSTN-IV [13, 14]. This is a tokamak with a high resistive cold plasma. The typical dimensionless parameters are $\eta_p = 1.4 \times 10^{-4}$, $V_p \approx 1.6 \times 10^{-3}$ (for frequency 30 kHz), $x_0/a = 0.25$,

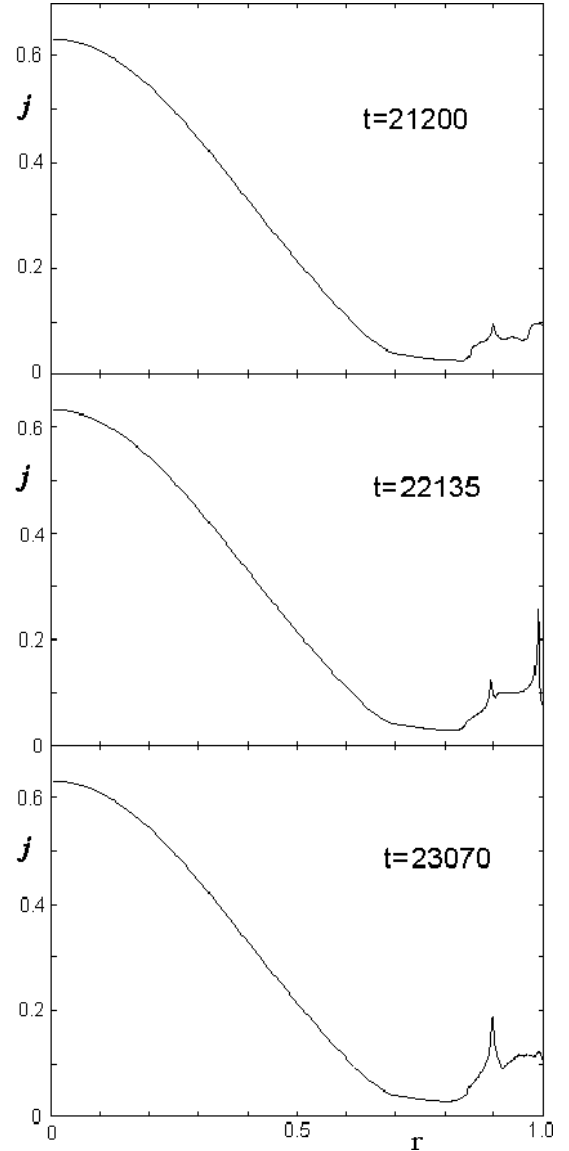


Figure 5. The distribution of j for the case of mixture of harmonics at different moments of time.

$r_c/a = 1.05$, $R_0/a = 4$, $m/n = 6/1$, $I_0 \text{ (kA)}/I_p \text{ (kA)} = 0.07/1$, the number of the coil $ml_0 = 24$. The coil are placed around torus. The two-dimensional approach describes correctly the coil geometry of CSTN-IV.

For the modelling of the device [13, 14] it is found that a stationary configuration is established in which the plasma rotates as a whole with the velocity $V_\phi = rV_p$ (except the boundary layer near $r = 1$ where V_ϕ tends to 0).

According to results of [13, 14], both numerical and experimental, an amplification of the coil magnetic field is observed in the plasma during the stationary phase. This is in contrast to our calculations, which show that the distribution of magnetic field perturbation during the stationary stage is close to the vacuum one which means that the amplification is negligible.

The authors of [13, 14] explain qualitatively the amplification by the properties of the equilibrium (pressure force compensates magnetic force) in the case of presence of resonance surface and azimuthal perturbation of the magnetic field. We can suggest another explanation of the amplification.

The main difference between our model and numerical model used in [13, 14] is that, in the latter, the resistivity is taken proportional to $T_e^{-3/2}$ where electron temperature T_e is calculated using the usual equation. Therefore, in [13, 14], η depends both on r and φ . In our opinion, the dependence of η on φ gives the amplification effect for the high resistive plasma.

Indeed, let us consider the stationary solution ($\partial V/\partial t = 0$, $\partial \psi/\partial t = -E_b$) of (3.1)–(3.4). We have

$$-E_b + (\mathbf{V}\nabla)\psi - V_p \frac{\partial \psi}{\partial \varphi} = \eta \left(\Delta \psi - \frac{2}{R} \right), \quad (6.1)$$

$$(\mathbf{V}\nabla)V_r - V_p \frac{\partial V_r}{\partial \varphi} = \frac{V_\varphi^2}{r} - \frac{\partial p}{\partial r} - \Delta \psi \frac{\partial \psi}{\partial r} + \nu \left(\Delta V_r - \frac{2}{r^2} \frac{\partial V_\varphi}{\partial \varphi} - \frac{V_r}{r^2} \right), \quad (6.2)$$

$$(\mathbf{V}\nabla)V_\varphi - V_p \frac{\partial V_\varphi}{\partial \varphi} = -\frac{V_r V_\varphi}{r} - \frac{1}{r} \frac{\partial p}{\partial \varphi} - \Delta \psi \frac{1}{r} \frac{\partial \psi}{\partial \varphi} + \nu \left(\Delta V_\varphi + \frac{2}{r^2} \frac{\partial V_r}{\partial \varphi} - \frac{V_\varphi}{r^2} \right). \quad (6.3)$$

For TEXTOR, η and E_b are small. Therefore according to (6.1), the values V_r , $V_\varphi - rV_p$ are small everywhere except for the thin boundary layer near $r = 1$, where $V_\varphi = 0$. The thickness of the boundary layer is very small because the viscosity in the hot TEXTOR plasma is very small ($\nu \ll \eta$). Therefore ψ doesn't change too much inside the boundary layer and we can say, that V_r , $V_\varphi - rV_p$ are close to zero everywhere. From this it follows, according to equations (6.2) and (6.3), that the distribution of the stationary magnetic field is close to immobile equilibrium:

$$\Delta \psi \nabla \psi = -\nabla p \quad (6.4)$$

and does not depend on η and V_p .

For the highly resistive CSTN-IV tokamak, the terms with η and E_b in (6.1) are not small. Therefore the stationary configuration will depend significantly on the resistivity. The deviation of ψ from the immobile equilibrium (6.4) will be large. From this it follows that the stationary velocity will be substantial.

The results of the solution of (3.1)–(3.4) shows that dependence resistivity on φ (we put a certain dependence 'by hand') can gives significant amplification of the coil magnetic field perturbation as in [13, 14]. However, the amplification decreases with η (with the same ratio $\eta/(\partial \eta/\partial \varphi)$). Our calculation also shows that the plasma velocity in the stationary phase increases with the resistivity. Note that in the case of TEXTOR this effect is small.

7. Conclusion

Our study shows that a stationary solution is established for a cylindrical plasma with a single harmonic external coils system; this is equivalent to a helicity with a single phase velocity. In this solution the plasma periphery rotates with a velocity $V_\varphi \approx rV_p$, while the plasma core remains immobile due to friction force connected with magnetic pumping and, to a smaller degree, with charge exchange effects. The distribution of magnetic field perturbation is consistent with the vacuum one.

This stationary configuration is achieved by passing through a configuration with a skin-sheet near the plasma edge and current sheet at the resonance surface. The plasma is accelerated rather quickly in this sheets. The duration of current sheet at the resonance surface amounts to about several hundred Alfvén times. This time duration is comparable with the period of a coil current perturbation. The building-up of the magnetic field configuration close to the stationary one in the DED case takes several tens thousand Alfvén times and depends strongly and nonlinearly on the amplitude of the coil current. For a small amplitude the duration is much longer.

In the case of a mixture of harmonics, an oscillating solution with a period given by equation (5.1) is established on a large timescale. In this case, the current density on the plasma periphery is rather high. The external magnetic field is significantly shielded inside plasma. The local velocity is significant different from its average value. This means that in real three-dimensional geometry the acceleration of the plasma in the poloidal direction does not provide a complete penetration of magnetic field perturbation. The magnetic field close to vacuum one is established only when plasma starts to rotate in toroidal direction with a velocity $R_0\omega/n$.

The toroidal acceleration of the plasma takes much longer than poloidal one, because the magnetic force in toroidal direction is an order of magnitude smaller than in the poloidal one. Therefore, the friction force, which does not depend on the poloidal acceleration of the plasma, can be important for the plasma acceleration in toroidal direction. The modelling of the toroidal acceleration in the DED case demands more sophisticated three-dimensional RMHD models such as [16], which can take toroidal plasma velocity into account.

Acknowledgments

The work was supported by the German government under the WTZ number RUS 00/572.

Appendix. The boundary conditions for magnetic flux

Here we obtain the formula (suggested by H J de Blank) for the boundary condition for ψ , which corresponds to continuity of ψ and $\partial \psi/\partial r$ between plasma and vacuum region.

Let us present ψ in a vacuum region as a sum of the vector potential of the coils in vacuum (without plasma) ψ_c and a function $\tilde{\psi}$, which corresponds to a solution of the equation for vector potential in vacuum $\Delta \tilde{\psi} = 0$.

$$\psi = \psi_c + \tilde{\psi}.$$

In the case of discretization of the poloidal angle with an equidistant grid $\varphi_j = 2\pi j/j_0$ ($j = 1, \dots, j_0$) we can expand $\tilde{\psi}$ in a discrete Fourier series. Due to the condition $\Delta \tilde{\psi} = 0$ we can write

$$\psi = \psi_c + a \ln r + c_0 + c_{(j_0/2)} r^{-j_0/2} (-1)^j + \sum_{m=1}^{j_0/2-1} r^{-m} \left[c_m \cos\left(\frac{2\pi m j}{j_0}\right) + s_m \sin\left(\frac{2\pi m j}{j_0}\right) \right]. \quad (A1)$$

Inside the plasma ($r < 1$) we introduce the discretization in r with index i . We apply the conditions that $r_{i_0} = 1$ and

$r_{i0-1} = 1 - h_r$. Using the approximation $\partial\psi/\partial r|_{r=1} = (\psi_{i0} - \psi_{i0-1})/h_r$ and formula (A1) the condition of the continuity of ψ and $\partial\psi/\partial r$ can be written as

$$\psi_{i0,j} = \psi_c + c_0 + c_{(j_0/2)}(-1)^j + \sum_{m=1}^{j_0/2-1} \left[c_m \cos\left(\frac{2\pi mj}{j_0}\right) + s_m \sin\left(\frac{2\pi mj}{j_0}\right) \right], \quad (\text{A2})$$

$$\frac{\psi_{i0,j} - \psi_{i0-1,j}}{h_r} = \frac{\partial\psi_c}{\partial r} + a - \frac{j_0}{2} c_{(j_0/2)}(-1)^j - \sum_{m=1}^{j_0/2-1} m \left[c_m \cos\left(\frac{2\pi mj}{j_0}\right) + s_m \sin\left(\frac{2\pi mj}{j_0}\right) \right]. \quad (\text{A3})$$

There are $2j_0+1$ unknown values a, c_m ($m = 0, \dots, j_0/2$), s_m ($m = 1, \dots, j_0/2 - 1$), $\psi_{i0,j}$ ($j = 1, \dots, j_0$) and $2j_0$ equations. The $(2j_0 + 1)$ st equation in the case of a straight cylinder cannot be found using only the information about plasma and coils current. It connected with an external parameter. In our case we assume that there is an electric field supporting the initial distribution of the plasma current. So

$$\frac{1}{2\pi} \int_0^{2\pi} \psi \, d\varphi = -E_b t.$$

Respectively, using (A2) we obtain

$$c_0 = -E_b t - \frac{1}{j_0} \sum_{m=1}^{j_0} \psi_{cj}. \quad (\text{A4})$$

Using (A2), we can write, by usual Fourier analysis,

$$c_{(j_0/2)} = \langle \psi_{i0} - \psi_c \rangle_{(j_0/2)}, \quad c_m = \langle \psi_{i0} - \psi_c \rangle_{c,m}, \\ s_m = \langle \psi_{i0} - \psi_c \rangle_{s,m}, \quad m = 1, \dots, j_0/2 - 1.$$

Substituting these coefficients into (A3) we will obtain

$$\frac{\psi_{i0,j} - \psi_{i0-1,j}}{h_r} = \frac{\partial\psi_c}{\partial r} + a - \frac{j_0}{2} \langle \psi_{i0} - \psi_c \rangle_{(j_0/2)}(-1)^j - \sum_{m=1}^{j_0/2-1} m \left[\langle \psi_{i0} - \psi_c \rangle_{c,m} \cos\left(\frac{2\pi mj}{j_0}\right) + \langle \psi_{i0} - \psi_c \rangle_{s,m} \sin\left(\frac{2\pi mj}{j_0}\right) \right]. \quad (\text{A5})$$

The operators $\langle \dots \rangle$ means the following

$$\langle f \rangle = j_0^{-1} \sum_{j=1}^{j_0} f_j, \quad \langle f \rangle_{(j_0/2)} = j_0^{-1} \sum_{j=1}^{j_0} (-1)^j f_j, \\ \langle f \rangle_{c,m} = \left(\frac{2}{j_0} \right) \sum_{j=1}^{j_0} f_j \cos\left(\frac{2\pi mj}{j_0}\right), \\ \langle f \rangle_{s,m} = \left(\frac{2}{j_0} \right) \sum_{j=1}^{j_0} f_j \sin\left(\frac{2\pi mj}{j_0}\right).$$

Substituting the expression for operators $\langle \dots \rangle$ we obtain from (A5)

$$\frac{\psi_{i0,j} - \psi_{i0-1,j}}{h_r} = \frac{\partial\psi_c}{\partial r} + a - \frac{1}{2} \sum_{k=1}^{j_0} (\psi_{i0,k} - \psi_c) (-1)^{k-j} - \sum_{m=1}^{j_0/2-1} \frac{2m}{j_0} \sum_{k=1}^{j_0} (\psi_{i0,k} - \psi_c) \cos\left(\frac{2\pi(k-j)m}{j_0}\right)$$

or

$$\frac{\psi_{i0,j} - \psi_{i0-1,j}}{h_r} = \frac{\partial\psi_c}{\partial r} + a - \sum_{k=1}^{j_0} Q(k-j)(\psi_{i0,k} - \psi_c). \quad (\text{A6})$$

Taking into account (A4) we can rewrite (A6) in the form (3.6).

Note, that the eigenfunctions of operator $\sum_{k=1}^{j_0} Q(k) f_{j+k}$ are $\exp(2\pi i j m / j_0)$ ($i^2 = -1$) has the m eigenvalues:

$$\sum_{k=1}^{j_0} Q(k) \exp\left(\frac{2\pi i (j+k)m}{j_0}\right) = m \exp\left(\frac{2\pi i j m}{j_0}\right).$$

Therefore, $\sum_{k=1}^{j_0} Q(k) = 0$.

References

- [1] Finken K.H. and Wolf G.H. 1997 *Fusion Eng. Des.* **37** 337
- [2] Finken K.H. 1997 *Nucl. Fusion* **37** 583
- [3] Kaleck A., Hassler M. and Evans T. 1997 *Fusion Eng. Des.* **37** 353
- [4] Abdullaev S.S., Eich Th. and Finken K.H. 2001 *Phys. Plasmas* **8** 2739
- [5] Abdullaev S.S., Finken K.H., Kaleck A. and Spatschek K.H. 1998 *Phys. Plasmas* **5** 196
- [6] Abdullaev S.S., Finken K.H., Kaleck A. and Spatschek K.H. 1999 *Phys. Plasmas* **6** 153
- [7] Kobayashi M., Sewell G., Finken K.H., Eich Th., Reiser D. and Abdullaev S.S. 2002 *Contrib. Plasma Phys.* **42** 163
- [8] Abdullaev S.S. and Spatschek K.H. 1999 *Phys. Rev. E* **60** 6287
- [9] Faulconer D.W. and Koch R. 1997 *Fusion Eng. Des.* **37** 399
- [10] Jensen T.H. 1997 *Fusion Eng. Des.* **37** 437
- [11] Finken K.H., Abdullaev S.S., Eich T., Faulconer D.W., Kobayashi M., Koch R., Mank G. and Rogister A. 2001 *Nucl. Fusion* **41** 503
- [12] Finken K.H. 1999 *Nucl. Fusion* **39** 707
- [13] Kobayashi M., Kojima H., Zhai K. and Takamura S. 2000 *Phys. Plasmas* **7** 3288
- [14] Kobayashi M., Tuda T., Tashiro K., Kojima H., Zhai Kan and Takamura S. 2000 *Nucl. Fusion* **40** 181
- [15] Izzo R. et al 1983 *Phys. Fluids* **26** 2240
- [16] Zhukov V. 2001 *Plasma Phys. Rep.* **27** 591
- [17] Hassam A.B. and Kurlrud R.M. 1978 *Phys. Fluids* **21** 2271
- [18] Gray D.S. et al 1998 *Nucl. Fusion* **38** 1585
- [19] Elfimov A.G., Petrzilka V. and Tataronis J.A. 1994 *Phys. Plasmas* **1** 2882
- [20] Fitzpatrick R. 1998 *Phys. Plasmas* **5** 3325